Nypa fruticans Wurmb inhibits melanogenesis in isobutylmethylxanthine-treated melanoma via the PI3K/AKT/mTOR/CREB and MAPK signaling pathways

SO-YEON HAN[1*], TAE-WON JANG[2*], HYE-JEONG PARK[1], SUNG-SOO OH[3],
JUNG-BOK LEE[4], SUNG-MIN MYOUNG[5] and JAE-HO PARK[2]

[1]Department of Medicinal Plant Science; [2]Department of Pharmaceutical Science, Jungwon University, Goesan-gun,
Chungcheongbuk-do 28024; [3]Research Center, Kiposs Co., Ltd., Seoul 08584; [4]Research and Innovation Center,
Kyochon Food and Beverage Co., Ltd., Hwaseong-si, Gyeonggi-do 18469; [5]Department of Public Health Administration,
Jungwon University, Goesan-gun, Chungcheongbuk-do 28024, Republic of Korea

Abstract. Malignant melanoma is responsible for 3.0 and 1.7% of cases of tumor incidence and tumor-associated mortality, respectively, in the Caucasian population. Melanoma is a type of skin cancer that occurs when melanocytes mutate and divide uncontrollably. *Nypa fruticans* Wurmb (NF) is abundant in phytochemicals (polyphenols and flavonoids) and is traditionally used to treat diseases of the respiratory tract. The present study investigated the inhibitory effect of the ethyl acetate fraction of NF (ENF) on melanogenesis-related factors in isobutylmethylxanthine-treated B16F10 melanoma cells. Phenolics and flavonoids (caffeic acid, catechin, epicatechin and hirsutine) in ENF were analyzed via liquid chromatography-mass spectrometry. In addition, the main factors involved in melanogenesis were identified using immunoblotting, reverse transcription-polymerase chain reaction (RT-PCR), RT-quantitative PCR and immunofluorescence. ENF significantly suppressed the expression of tyrosinase (TYR) and TYR-related proteins 1 and 2 (TYRP-1/2), which are the main factors involved in melanogenesis. ENF also inhibited the expression of microphthalmia-associated transcription factor (MITF) by phosphorylating the related cell signaling proteins (protein kinase B, mammalian target of rapamycin, phosphoinositide 3-kinase and cAMP response element-binding protein). Furthermore, ENF inhibited the phosphorylation of extracellular signal-regulated kinase and thereby downregulated melanogenesis. In conclusion, ENF inhibited melanogenesis by suppressing MITF, which controls TYRP-1/2 and TYR. These results suggested that ENF may be a natural resource that can inhibit excessive melanin expression by regulating various melanogenesis pathways.

Introduction

The expression of melanin, which produces pigmentation (hair or skin color), is regulated by tyrosinase (TYR) and tyrosinase-related proteins 1 and 2 (TYRP-1/2) (1,2). TYR is regulated by microphthalmia-associated transcription factor (MITF), which mediates the growth, proliferation, and differentiation of melanocytes (3). MITF is regulated by several cell signaling pathways during melanogenesis (4,5). Stimulants such as isobutylmethylxanthine (IBMX), α-melanotropin, and forskolin activate melanogenesis-related proteins by inducing the expression of MITF and cyclic adenosine monophosphate (cAMP) (6,7). Melanogenesis-related proteins are activated by cAMP response element-binding protein (CREB), which is phosphorylated by protein kinase A, thereby promoting MITF transcription and inducing eumelanin synthesis (8-10). MITF expression is regulated via the protein kinase B (AKT), extracellular signal-regulated kinase (ERK), and phosphoinositide 3-kinase (PI3K) signaling pathways during melanogenesis (11). Phosphorylated ERK (p-ERK), AKT (p-AKT), and PI3K (p-PI3K) inhibit melanin activity by promoting the degradation and phosphorylation of MITF (12,13). *Nypa fruticans* Wurmb (NF) is a plant found primarily in tropical mangrove systems (14). NF is considered a plant with low utility in the Araceae family. Its roots, leaves, and stems have been traditionally used as analgesics for liver disease, asthma, and sore throat (15). NF contains several substances (such as flavonoids and polyphenols) that reportedly exhibit anticancer and antioxidative effects (16). In addition, flavonoids and polyphenols present in plants reportedly inhibit melanogenesis (17-20). Studies have indicated that NF has anti-nociceptive, neuroprotective, and anti-inflammatory properties (21,22). Therefore,

Correspondence to: Professor Jae-Ho Park, Department of Pharmaceutical Science, Jungwon University, 85 Munmu-ro, Goesan-gun, Chungcheongbuk-do 28024, Republic of Korea
E-mail: parkjh@jwu.ac.kr

*Contributed equally

we investigated the inhibitory effect of the ethyl acetate fraction of *N. fruticans* (ENF) on melanogenesis and cell signaling pathways via AKT/mammalian target of rapamycin (mTOR)/CREB and mitogen-activated protein kinase (MAPK).

Materials and methods

Chemicals and reagents. HPLC-grade petroleum ether, methanol, dimethyl sulfoxide (DMSO), and ethyl acetate were purchased from Merck (Darmstadt, Germany). Antibiotics (streptomycin and penicillin), 0.25% trypsin with EDTA in HBSS, high-glucose Dulbecco's modified Eagle medium (DMEM), and fetal bovine serum (FBS) were purchased from Biowest (Nuaillé, France). Plasmocin prophylactic for mycoplasma growth inhibition was purchased from InvivoGen (San Diego, CA, USA). Antibodies for TYR (SC-7834), TYRP-1 (SC-10448), TYRP-2 (SC-10451), and MITF (SC-10999) and anti-goat antibodies (SC-2020) were purchased from Santa Cruz Biotechnology (Dallas, TX, USA). p-ERK (9101S), ERK (4695S), p-CREB (9198S), CREB (4820S), p-AKT (4060S), AKT (9272S), p-mTOR (5536S), mTOR (2972S), PI3K (4292S), and anti-mouse (7076S) and anti-rabbit (7074S) antibodies were purchased from Cell Signaling (Danvers, MA, USA). Glyceraldehyde 3-phosphate dehydrogenase (GAPDH, ab8245), Alexa Fluor® 568 (ab175471), p-PI3K (ab182651), and Alexa Fluor® 488 (ab150113) were purchased from Abcam (Cambridge, MA, USA). All standards for chromatography were purchased from Sigma-Aldrich (St. Louis, MO, USA).

Sample preparation. NF was purchased from Nesta (Dongdaemun-gu, Seoul, Korea). An NF sample (484.0 g) was extracted with 80% methanol (4.2 l) for 7 days. The extract and fraction were concentrated using a vacuum evaporator (N-1110S, EYELA, Tokyo, Japan). The aqueous residue was fractionated with petroleum ether and ethyl acetate. The fractionated sample (ENF, 36.8 g) was refrigerated at 4°C until use. ENF used in the experiment was dissolved in DMSO (not exceeding 0.1%) at a concentration of 50 mg/ml.

Analysis of compounds in ENF using liquid chromatography-mass spectrometry (LC-MS). Compounds in ENF (injection volume: 10 μl) were analyzed using an e2695 system equipped with an ACQUITY QDa detector (Waters, Milford, MA, USA) based on standards. The column used for separation, a Sunfire (C18, 5 μm, 250x4.6 mm, Waters), was maintained at 25°C during analysis. 100% Acetonitrile (solvent A) and 1.0% glacial acetic acid in deionized water (solvent B) were used as solvents for the mobile phase (flow rate: 0.3 ml/min). The proportions of solvent A were set as 1.0% at 0 min, 20% at 8 min, 30% at 40 min, 40.0% at 45 min, and 1.0% at 50 min. The electrospray ionization mass spectrometer was operated in the negative ion mode (mass range: m/z 100-600). The cone voltage was set to 30 V and the capillary voltage was set to 0.8 kV.

Cell culture. B16F10 cells were purchased from the American Type Culture Collection (CRL-6475, Manassas, VA, USA). The cells were grown in an incubator (Thermo

Table I. Primer sequences for RT-PCR and RT-qPCR.

A, RT-PCR

Gene	Sequence, 5'-3'	Product size, bp
TYR	F: GAGAAGCGAGTCTTGATTAG	176
	R: TGGTGCTTCATGGGCAAAATC	
TYRP-1	F: GCTGCAGGAGCCTTCTTTCTC	268
	R: AAGACGCTGCACTGCTGGTCT	
TYRP-2	F: CCTGTCTCTCCAGAAGTTTG	218
	R: CGTCTGTAAAAGAGTGGAGG	
MITF	F: AGCGTGTATTTTCCCCACAG	124
	R: TAGCTCCTTAATGCGGTCGT	
GAPDH	F: AACTTTGGCATTGTGGAAGG	130
	R: ATGCAGGGATGATGTTCTGG	

B, RT-qPCR

Gene	Sequence, 5'-3'	Product size, bp
TYR	F: ACAGCTACCTCCAAGAGTCA	148
	R: TACTGCTAAGCCCAGAGAGA	
TYRP-1	F: CAAAGAGCAGCATAGGAGAC	139
	R: ACACTCTCGTGGAAACTGAG	
TYRP-2	F: ATGAGGAGCTCTTCCTAACC	106
	R: CCAATGACCACTGAGAGAGT	
MITF	F: CTCAGCAGTCTCTTTTGGAC	110
	R: AATGTCTACAGAGGCACCAC	
GAPDH	F: CCTCCAAGGAGTAAGAAACC	143
	R: CTAGGCCCCTCCTGTTATTA	

F, forward; R, reverse; RT-PCR, reverse transcription-polymerase chain reaction; RT-qPCR, RT-quantitative PCR; TYR, tyrosinase; TYRP, TYR-related protein; MITF, microphthalmia-associated transcription factor; GAPDH, glyceraldehyde 3-phosphate dehydrogenase.

Fisher Scientific, Waltham, MA, USA) under 5% CO_2 in a humidified environment at 37°C. The medium for cell culture consisted of DMEM containing 1% antibiotics, 1 ml Plasmocin prophylactic, and 10% FBS (complete DMEM: cDMEM).

Cell viability using MTS assay. The protocol used in a previous study was adopted (23). Briefly, cell viability was measured using MTS reagent (Cell Titer 96® Aqueous One Solution, Promega, Madison, WI, USA). B16F10 cells were cultured in a 96-well plate using cDMEM for 24 h. The cells were treated with ENF (12.5-400.0 μg/ml) for 24 h. Next, they were treated with 20 μl MTS reagent for 2 h in an incubator maintained with 5% CO_2 in a humidified environment at 37°C. The absorbance of MTS reagent at a wavelength of 540 nm was measured using a microplate reader (Biotek, Winooski, VT, USA) to determine cell viability.

Table II. Catechin, epicatechin, and isoquercitrin content of ethyl acetate fraction of *Nypa fruticans* Wurmb as determined by liquid chromatography-mass spectrometry analysis.

Compound	Molecular weight	Retention time, min	Content, mg/g
Catechin	290.26	24.751	130.1
Epicatechin	290.26	26.991	16.1
Isoquercitrin	464.10	35.164	85.7

Measurement of melanin content. The modified protocol used in a previous study was adopted (24). Briefly, the melanin content at the cellular level was investigated. B16F10 cells were treated with ENF and IBMX for 48 h. The melanin produced was dissolved in 1 N NaOH containing 10% DMSO at 80˚C and the absorbance of the solution was measured at 475 nm using a UV/Visible spectrophotometer (X-ma 3000 (PC), Human Corp., Seoul, Korea).

Immunoblotting. B16F10, the murine skin melanoma cell line, was cultured at a density of $2x10^5$ cells/well in a 6-well plate for 24 h. Cells were pre-treated with ENF (25.0, 50.0, and 100.0 μg/ml) for 2 h and then treated with IBMX for 48 h. The cell lysates prepared using RIPA buffer (supplemented with protease inhibitor cocktail and 0.5 M EDTA solution, Thermo Fisher Scientific) were centrifuged at 16,000 x g and 4˚C for 15 min. Protein content in the cell lysates was quantified using Quick Start Bradford 1X Dye Reagent (Bio-Rad, Hercules, CA, USA) following the manufacturer's protocol. The proteins were electrophoresed and then transferred to polyvinylidene fluoride membranes (Bio-Rad) using the Trans-Blot® Turbo™ Transfer System (Bio-Rad). Blots were blocked using 5.0% BSA (Bovine Serum Albumin , Bio-Sesang, Seoul, Korea) in Tris-buffered saline supplemented with 0.1% Tween 20 (TBS-T, Bio-Sesang). Next, a specific primary antibody was added to 3.0% BSA (1:2,000) and incubated overnight at 4˚C. Subsequently, the blots were washed with TBS-T and incubated with the HRP-conjugated secondary antibody for 1 h. Chemiluminescence was detected using Clarity™ Western ECL substrate (Bio-Rad) and visualized with a Chemi-Doc (Bio-Rad). The intensity of the blots was analyzed using ImageJ software 1.51k (developed at the National Institutes of Health, USA).

cDNA synthesis, reverse transcription-quantitative polymerase chain reaction (RT-qPCR), and reverse transcription-polymerase chain reaction (RT-PCR). cDNA was synthesized from extracted RNA using NucleoSpin® RNA Plus (Macherey-Nagel, Düren, Germany) in a T100™ thermal cycler (Bio-Rad) according to the user manual. RT-qPCR was performed using a Rotor-Gene Q (Qiagen, Hilden, Germany) with a QuantiTect® SYBR Green PCR kit (Qiagen) and an appropriate primer according to the user manual. Primer 3 software was used for primer design (Table I). Data analysis was conducted using Rotor-Gene Q Series software 2.3.5 (Qiagen). Transcription levels were normalized to those of the *GAPDH* gene. The formula used to analyze mRNA expression was $2^{-\Delta\Delta Ct}$, where $\Delta\Delta Ct=(Ct_{target}-Ct_{GAPDH})_{sample}-(Ct_{target}-Ct_{GAPDH})_{control}$. RT-PCR was performed using a T100™ thermal cycler with Quick Taq® HS DyeMix (Toyobo, Osaka, Japan) and synthesized cDNA. The PCR product was subjected to DNA electrophoresis (2% agarose gel with DNA SafeStain, LAMDA Biotech, Ballwin, MO, USA). The intensity of the bands was analyzed using ImageJ software.

Immunofluorescence (IF). B16F10 cells were cultured on a glass coverslip and incubated for 24 h. The cells were pre-treated with ENF (100 μg/ml) for 2 h and then treated with IBMX for 24 h. Thereafter, the cells were treated with 4% para-formaldehyde (Bio-Sesang) dissolved in phosphate-buffered saline (PBS) and incubated at 25˚C for 15 min for fixing. After incubation, the cells were washed with PBS and blocked with 2% BSA in PBS (supplemented with 0.1% Triton-X, PBS-T, Bio-Sesang) for 1 h. For IF analysis, the coverslips were treated with anti-TYR and MITF antibodies (diluted 1:1,000) in 1% BSA/PBS-T and incubated overnight at 4˚C. After incubation, anti-goat IgG (Alexa Fluor® 568) and anti-mouse IgG (Alexa Fluor® 488) were reacted with the primary antibody and incubated for 1 h in the dark. 4',6-Diamidino-2-phenylindole (Invitrogen, Waltham, MA, USA) was diluted in PBS-T and incubated at 25˚C for 10 min. A fluorescence mounting solution (S3023, Dako, Carpinteria, CA, USA) was added to the slide to mount the coverslip. Images at x400 magnification were captured using a fluorescence microscope (CKX53, Olympus, Tokyo, Japan) and DSLR camera (DS126271, Canon, Tokyo, Japan), and the fluorescence intensity was analyzed using ImageJ software.

Statistical analysis. All experimental data were statistically analyzed using a statistics program (GraphPad Prism 5.02, GraphPad Software, San Diego, CA, USA). Each data point was analyzed using one-way analysis of variance. Dunnett's post-hoc test was used to compare mean values between groups. $P<0.05$ was considered to indicate a statistically significant difference.

Results

Compound analysis. The compounds in ENF were identified using LC-MS chromatograms and quantified by comparison with the quantitative linear equations of the corresponding standards. The quantitative linear equation and its linearity for catechin (y=12434x+276633, R^2=0.9917), epicatechin (y=11765x+412542, R^2=0.9865), and isoquercitrin (y=21534x-700748, R^2=0.9945) were determined using various concentrations of the standards (Fig. 1). Thus, it was found that ENF contained 130.1 mg/g of catechin, 16.1 mg/g of epicatechin, and 85.7 mg/g of isoquercitrin (Table II).
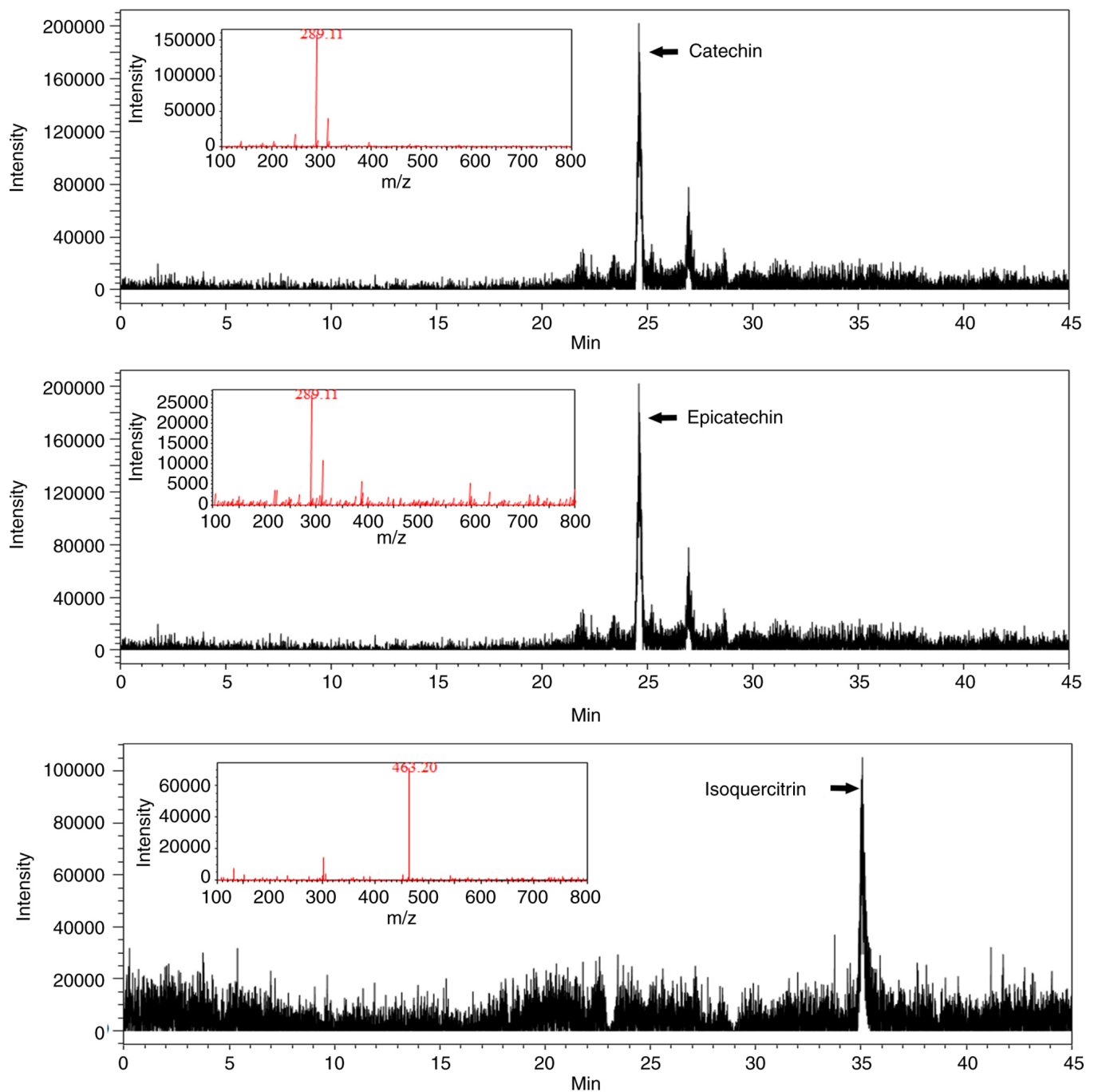
Figure 1. Liquid chromatography-mass spectrometry analysis of catechin, epicatechin, and isoquercitrin contents of ethyl acetate fraction of *Nypa fruticans* Wurmb.

Effects of ENF on cell viability. To investigate the cytotoxicity of ENF, B16F10 cells were treated with 0-400 μg/ml ENF and incubated for 24 h. After incubation, MTS reagent was used to analyze cell viability following the manufacturer's protocol. ENF did not significantly inhibit cell growth and exhibited no cytotoxicity in B16F10 cells up to a concentration of 400 μg/ml (Fig. 2).

Effects of ENF on the expression of TYR, TYRP-1, TYRP-2, and MITF. To evaluate whether ENF inhibits melanogenesis, we measured intracellular melanin contents after the application of ENF to B16F10 cells in the presence of IBMX. As shown in Fig. 3A, IBMX treatment increased intracellular melanin
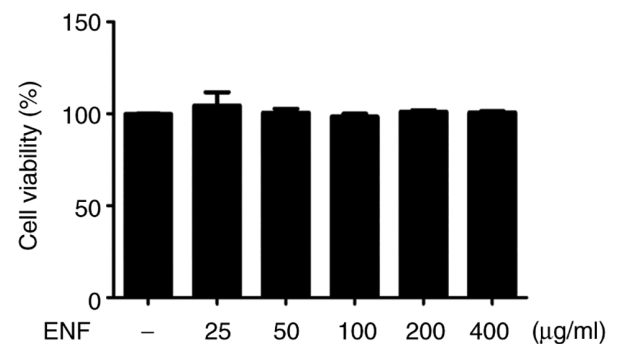

Figure 2. Viability of B16F10 cells after ENF treatment. ENF, ethyl acetate fraction of *Nypa fruticans* Wurmb.
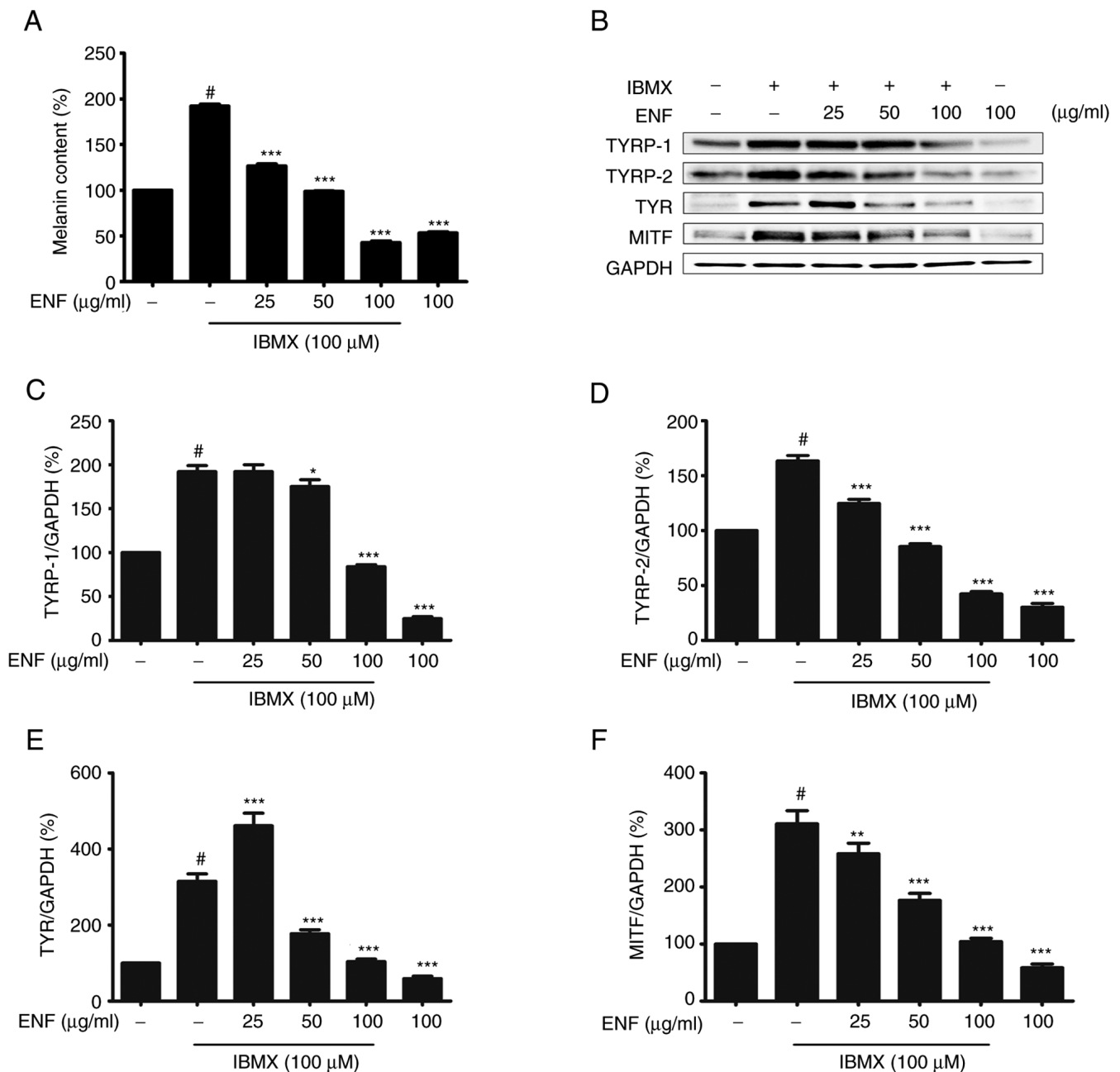
Figure 3. Inhibitory effects of ENF on the expression of melanin, TYRP-1, TYRP-2, TYR, and MITF during melanogenesis. (A) Effect of ENF on melanin content in B16F10 cells. (B) Expression of TYRP-1, TYRP-2, TYR, and MITF based on immunoblotting. (C) Bar graph of TYRP-1 expression. (D) Bar graph of TYRP-2 expression. (E) Bar graph of TYR expression. (F) Bar graph of MITF expression. All results are expressed as means ± standard deviations (n≥3). #P<0.001 vs. untreated group; *P<0.05, **P<0.01, ***P<0.001 vs. IBMX-stimulated group. ENF, ethyl acetate fraction of *Nypa fruticans* Wurmb; IBMX, isobutylmethylxanthine; MITF, microphthalmia-associated transcription factor; TYR, tyrosinase; TYRP, TYR-related protein.

contents compared with those of the control. However, ENF treatment in the presence of IBMX decreased intracellular melanin contents compared with those of the IBMX-treated group. B16F10 cells stimulated by IBMX exhibited an increase in the expression of TYRP-1 (1.86-fold), TYRP-2 (1.62-fold), TYR (3.03-fold), and MITF (2.96-fold) compared with the untreated group (1.00-fold). In contrast, ENF treatment alone at 50 and 100 µg/ml significantly decreased the expression of TYRP-1 (1.69 and 0.83-fold), TYRP-2 (0.86 and 0.44-fold), TYR (1.73 and 1.04-fold), and MITF (1.73 and 1.04-fold) (Fig. 3B-F). The inhibitory effect of ENF was also confirmed at the mRNA level (Fig. 4A-E). B16F10 cells stimulated by IBMX

exhibited an increase in the expression of TYRP-1 (3.62-fold), TYRP-2 (3.07-fold), TYR (2.45-fold), and MITF (3.02-fold) mRNA compared with the untreated group (1.00-fold). ENF treatment at 100 µg/ml suppressed the mRNA levels of TYRP-1 (2.14-fold), TYRP-2 (2.40-fold), TYR (1.80-fold), and MITF (1.80-fold). The accumulation of TYR and MITF in live cells was confirmed using immunofluorescence (Fig. 5A-C). TYR (green) over-accumulated in the IBMX-treated group. Its accumulation was suppressed in the 100 µg/ml ENF-treated group. MITF (red) also showed excessive accumulation in the IBMX-treated group; its accumulation was also suppressed in the 100 µg/ml ENF-treated group.
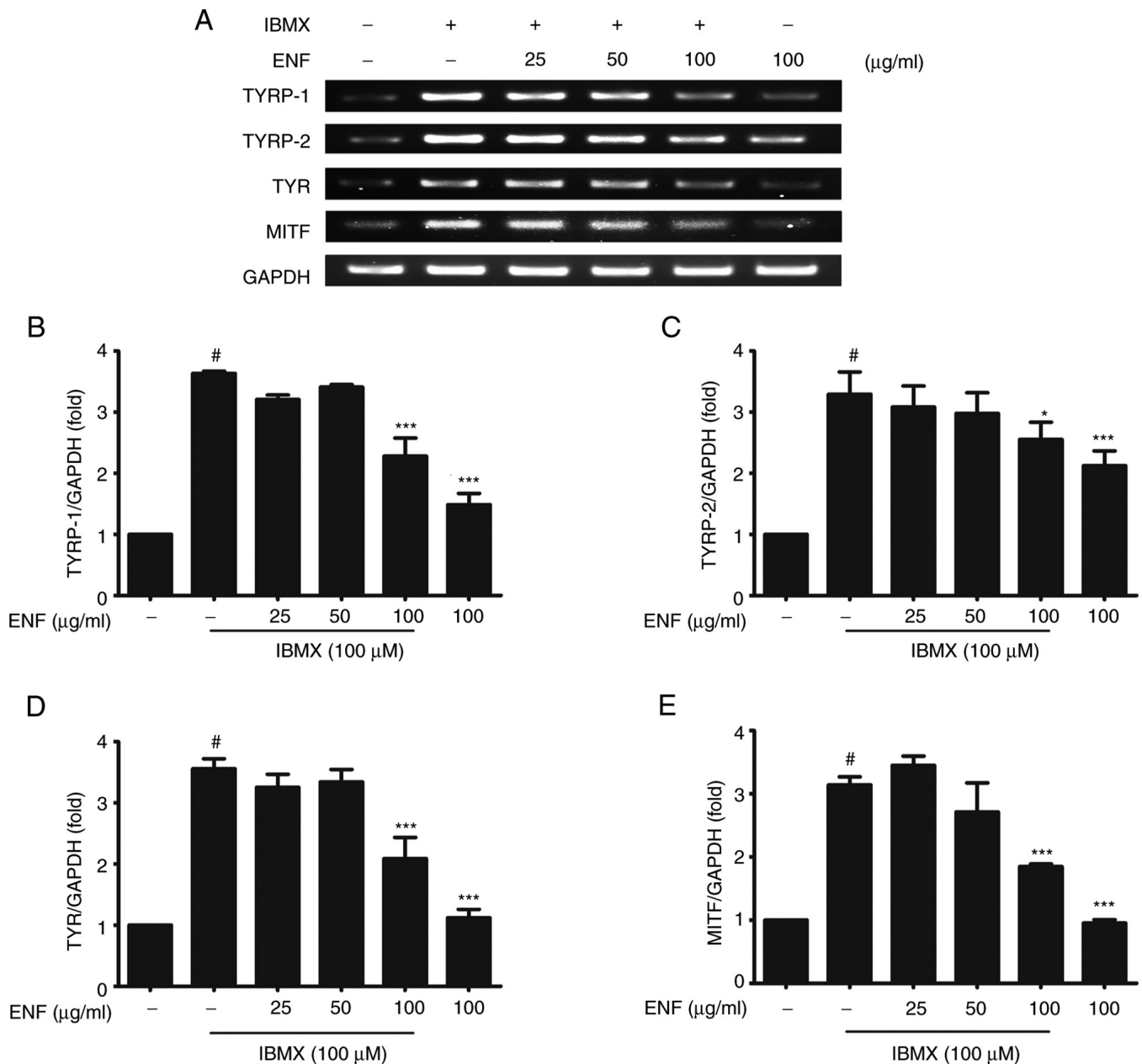
Figure 4. Inhibitory effects of ENF on expression of TYRP-1, TYRP-2, TYR, and MITF mRNA during melanogenesis. (A) Expression of TYRP-1, TYRP-2, TYR, and MITF mRNA based on RT-PCR. (B) Bar graph of the expression of TYRP-1 mRNA based on RT-qPCR. (C) Bar graph of the expression of TYRP-2 mRNA based on RT-qPCR. (D) Bar graph of the expression of TYR mRNA based on RT-qPCR. (E) Bar graph of the expression of MITF mRNA based on RT-qPCR. All results are expressed as means ± standard deviations (n≥3). #$P<0.001$ vs. untreated group; *$P<0.05$, ***$P<0.001$ vs. IBMX-stimulated group. ENF, ethyl acetate fraction of *Nypa fruticans* Wurmb; IBMX, isobutylmethylxanthine; MITF, microphthalmia-associated transcription factor; RT-PCR, reverse transcription-polymerase chain reaction; RT-qPCR, RT-quantitative PCR; TYR, tyrosinase; TYRP, TYR-related protein.

Effects of ENF on CREB and PI3K/AKT/mTOR signaling pathways. The CREB and PI3K/AKT/mTOR signaling pathways reportedly regulate MITF expression (25-29). B16F10 cells stimulated by IBMX showed an increase in the expression of p-CREB (1.68-fold) compared with the untreated group (1.00-fold). The p-CREB levels were lower in the ENF-treated groups (0.08-fold at 100 µg/ml) than in the IBMX-stimulated group (Fig. 6A and B). In IBMX-induced B16F10 cells, the levels of mTOR, AKT, and PI3K phosphorylation were 3.42, 4.58, and 1.29-fold higher than those in the untreated group (1.00-fold). In contrast, mTOR, AKT, and PI3K showed lower phosphorylation levels in the ENF-treated group (0.16, 0.75,

and 0.10-fold at 100 µg/ml) than in the IBMX-stimulated group (Fig. 6A-E). Finally, ERK phosphorylation was significantly inhibited in the ENF-treated group (0.67-fold at 100 µg/ml) compared with that in the IBMX-stimulated group (1.26-fold) (Fig. 6A and F).

Discussion

Melanin protects the dermis, hypodermis, and epidermis from external stimuli; however, when produced in excess, it causes various problems, such as hyperpigmentation, freckles, and skin cancer (30). This study revealed that
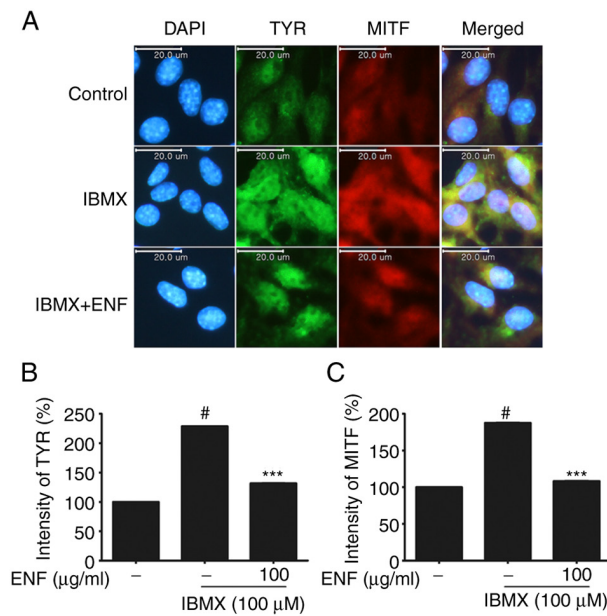
Figure 5. Immunofluorescence analysis of TYR and MITF against ENF. (A) Immunofluorescence image from fluorescence microscope. (B) Bar graph of TYR immunofluorescence. (C) Bar graph of MITF immunofluorescence. Micrographs were taken using a fluorescence microscope (magnification, x400). #P<0.001 vs. untreated group; ***P<0.001 vs. IBMX-stimulated group. ENF, ethyl acetate fraction of *Nypa fruticans* Wurmb; IBMX, isobutylmethylxanthine; MITF, microphthalmia-associated transcription factor; TYR, tyrosinase.
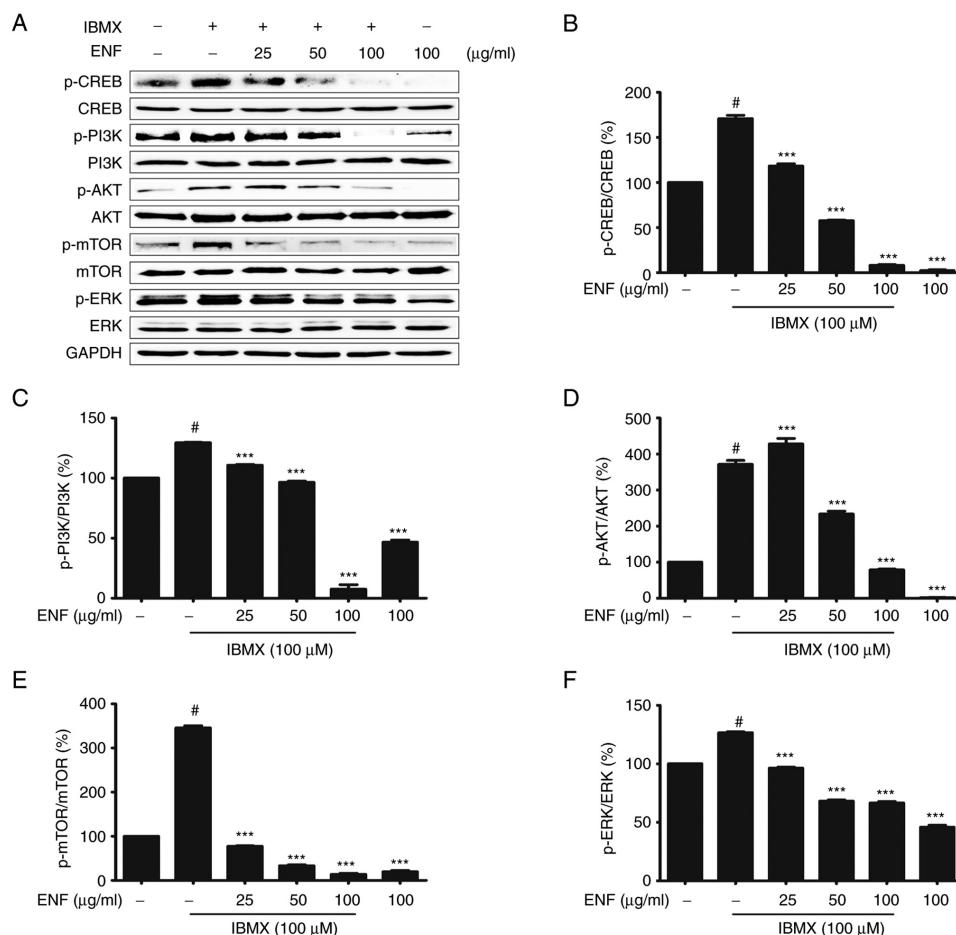

Figure 6. Inhibitory effects of ENF on the expression of p-CREB, p-PI3K, p-AKT, p-mTOR, and p-ERK during melanogenesis. (A) Expression of p-CREB, p-PI3K, p-AKT, p-mTOR, and p-ERK based on immunoblotting. (B) Bar graph of p-CREB expression. (C) Bar graph of p-PI3K expression. (D) Bar graph of p-AKT expression. (E) Bar graph of p-mTOR expression. (F) Bar graph of p-ERK expression. All results are expressed as means ± standard deviations (n≥3). #P<0.001 vs. untreated group; ***P<0.001 vs. IBMX-stimulated group. AKT, protein kinase B; CREB, cAMP response element-binding protein; ENF, ethyl acetate fraction of *Nypa fruticans* Wurmb; ERK, extracellular signal-regulated kinase; IBMX, isobutylmethylxanthine; mTOR, mammalian target of rapamycin; p-, phosphorylated; PI3K, phosphoinositide 3-kinase.

ENF inhibits melanogenesis in B16F10 cells. ENF treatment (25-100 μg/ml) decreased the melanin content at the cellular level in a dose-dependent manner. TYR is known as a rate-limiting enzyme essential for melanogenesis; a decrease in TYR levels leads to the inhibition of melanin production (31,32). Catechin, epicatechin, and isoquercitrin, which are phenolic compounds, regulate melanogenesis by inhibiting TYR (33-35). LC-MS analysis showed that ENF contains catechin (130 mg/g), epicatechin (16.1 mg/g), and isoquercitrin (85.7 mg/g). A previous study on catechin revealed its inhibitory effects on cell proliferation in melanoma and TYR expression (above 5 μM) (36). Moreover, catechin and epicatechin (each above 1.2 mg/ml) are known to inhibit the activities of enzymes related to melanin biosynthesis (37). ENF suppresses melanin production by regulating the expression of the proteins involved in melanogenesis (TYR, TYRP-1, TYRP-2, and MITF). This inhibition of melanogenesis-related factors can be attributed to the activities of phenolic compounds, such as isoquercitrin, catechin, and epicatechin. Isoquercitrin acts as a mediator that strongly inhibits melanogenesis (half-maximal inhibitory concentration: 21.7 μM) by suppressing TYR expression at the cellular level (38). These studies suggest that the levels of melanin, which is synthesized by TYR, are decreased by the activity of the phytochemicals in ENF, such as catechin, epicatechin, and isoquercitrin. In studies of other plants (*Pinellia pedatisecta*, *P. ternata*, and *Colocasia affinis*) belonging to the Araceae family, the bioactivity derived from the phytochemicals in these plants were found to regulate melanogenesis, inhibit cancer, and alleviate inflammation (39-41). The inhibitory effect of ENF on melanogenesis is related to cellular signaling pathways associated with MITF, which is controlled via PI3K/AKT/mTOR, ERK, and CREB (42). The inhibitory effect of ENF on phosphorylation in the signaling pathways induced by IBMX was confirmed based on the downregulation of the pathways by the phytochemicals in NF (40). It is assumed that this decrease in phosphorylation levels downregulates MITF expression via cell signaling transduction and inhibits melanin biosynthesis. Collectively, these findings indicated that PI3K/AKT/mTOR and CREB phosphorylation were inhibited. Hence, MITF inhibition via the downregulation of various signaling pathways is considered the mechanism by which ENF suppresses melanogenesis (Fig. 7). Although it is known that there are more factors (43-46) that exist in the mechanism of inhibiting melanogenesis, not clarifying some factors for eliciting effects on melanogenesis is considered a limitation of this study. However, by confirming the mechanism by which ENF inhibits MITF, the potential seen possibility that natural resources can be used academically and industrially as materials for anti-melanogenesis agents, cosmetics, food, and pharmaceuticals.
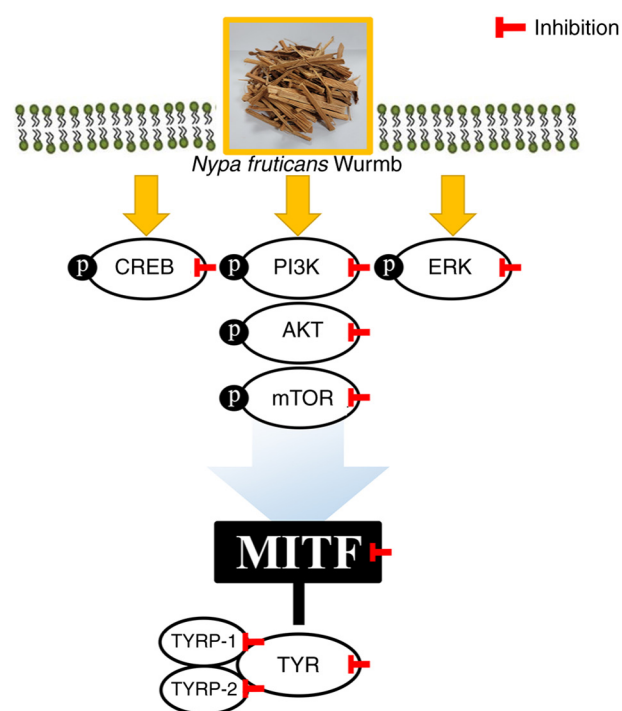

Figure 7. Effects of ENF on MITF inhibition. MITF was inhibited through various signaling pathways. ENF, ethyl acetate fraction of *Nypa fruticans* Wurmb; MITF, microphthalmia-associated transcription factor; p-CREB, phosphorylated cAMP response element-binding protein; p-PI3K, phosphorylated phosphoinositide 3-kinase; p-ERK, phosphorylated extracellular signal-regulated kinase; p-AKT, phosphorylated protein kinase B; p-mTOR, phosphorylated mammalian target of rapamycin; TYRP-1, TYR-related protein-1; TYRP-2, TYR-related protein-2; TYR, tyrosinase.

Availability of data and materials

The datasets used and/or analyzed during the current study are available from the corresponding author on reasonable request.

Authors' contributions

SYH and TWJ conceived the study and wrote the manuscript. SYH, TWJ and HJP performed the experiments. SYH, TWJ, JBL, SSO, SMM and JHP carried out the data collection and data analysis. SYH, TWJ, JHP, HJP, JBL, SSO and SMM confirm the authenticity of all the raw data. SYH, TWJ, JHP, HJP, JBL, SSO and SMM reviewed the results. All authors have read and approved the final manuscript.

Ethics approval and consent to participate

Not applicable.

Patient consent for publication

Not applicable.

Competing interests

The authors declare that they have no competing interests.

References

1. Gilchrest BA and Eller MS: DNA photodamage stimulates melanogenesis and other photoprotective responses. J Investig Dermatol Symp Proc 4: 35-40, 1999.
2. Swalwell H, Latimer J, Haywood RM and Birch-Machin MA: Investigating the role of melanin in UVA/UVB-and hydrogen peroxide-induced cellular and mitochondrial ROS production and mitochondrial DNA damage in human melanoma cells. Free Radic Biol Med 52: 626-634, 2012.
3. Buscà R and Ballotti R: Cyclic AMP a key messenger in the regulation of skin pigmentation. Pigment Cell Melanoma Res 13: 60-69, 2000.
4. Jiang Z, Xu J, Long M, Tu Z, Yang G and He G: 2,3,5,4'-Tetrahydroxystilbene-2-O-β-d-glucoside (THSG) induces melanogenesis in B16 cells by MAP kinase activation and tyrosinase upregulation. Life Sci 85: 345-350, 2009.
5. Ye Y, Chu JH, Wang H, Xu H, Chou GX, Leung AK, Fong WF and Yu ZL: Involvement of p38 MAPK signaling pathway in the anti-melanogenic effect of San-bai-tang, a Chinese herbal formula, in B16 cells. J Ethnopharmacol 132: 533-535, 2010.
6. Jung E, Lee J, Huh S, Lee J, Kim YS, Kim G and Park D: Phloridzin-induced melanogenesis is mediated by the cAMP signaling pathway. Food Chem Toxicol 47: 2436-2440, 2009.
7. Han HJ, Park SK, Kang JY, Kim JM, Yoo SK and Heo HJ: Anti-melanogenic effect of ethanolic extract of *Sorghum bicolor* on IBMX-induced melanogenesis in B16/F10 melanoma cells. Nutrients 12: 832, 2020.
8. Bertolotto C, Abbe P, Hemesath TJ, Bille K, Fisher DE, Ortonne JP and Bauotti R: Microphthalmia gene product as a signal transducer in cAMP-induced differentiation of melanocytes. J Cell Biol 142: 827-835, 1998.
9. Park WS, Kwon O, Yoon TJ and Chung JH: Anti-graying effect of the extract of *Pueraria thunbergiana* via upregulation of cAMP/MITF-M signaling pathway. J Dermatol Sci 75: 153-155, 2014.
10. Kang YG, Choi EJ, Choi Y and Hwang JK: 5,7-Dimethoxyflavone induces melanogenesis in B16F10 melanoma cells through cAMP-dependent signalling. Exp Dermatol 20: 445-447, 2011.
11. Jang JY, Lee JH, Kang BW, Chung KT, Choi YH and Choi BT: Dichloromethane fraction of *Cimicifuga heracleifolia* decreases the level of melanin synthesis by activating the ERK or AKT signaling pathway in B16F10 cells. Exp Dermatol 18: 232-237, 2009.
12. Jang JY, Kim HN, Kim YR, Choi WY, Choi YH, Shin HK and Choi BT: Partially purified components of *Nardostachys chinensis* suppress melanin synthesis through ERK and Akt signaling pathway with cAMP down-regulation in B16F10 cells. J Ethnopharmacol 137: 1207-1214, 2011.
13. Kim DS, Jeong YM, Park IK, Hahn HG, Lee HK, Kwon SB, Jeong JH, Yang SJ, Sohn UD and Park KC: A new 2-imino-1,3-thiazoline derivative, KHG22394, inhibits melanin synthesis in mouse B16 melanoma cells. Biol Pharm Bull 30: 180-183, 2007.
14. Cho JH, Robinson JP, Arave RA, Burnett WJ, Kircher DA, Chen G, Davies MA, Grossmann AH, VanBrocklin MW, McMahon M and Holmen SL: AKT1 activation promotes development of melanoma metastases. Cell Rep 13: 898-905, 2015.
15. Mantiquilla JA, Shiao MS, Lu HY, Sridith K, Sidique SN, Liyanage WK, Chu YL, Shih HC and Chiang YC: Deep structured populations of geographically isolated nipa (*Nypa fruticans* Wurmb.) in the Indo-West Pacific revealed using microsatellite markers. Frontiers in Plant Science 13, 2022.
16. Prasad N, Yang B, Kong KW, Sun J, Azlan A, Ismail A and Romi ZB: Phytochemicals and antioxidant capacity from *Nypa fruticans* Wurmb. fruit. Evid Based Complementary Altern Med: Article ID 154606, 9 pages: 2013.
17. Kim D, Park J, Kim J, Han C, Yoon J, Kim N, Seo J and Lee C: Flavonoids as mushroom tyrosinase inhibitors: A fluorescence quenching study. J Agric Food Chem 54: 935-941, 2006.
18. Kubo I and Kinst-Hori I: Flavonols from saffron flower: Tyrosinase inhibitory activity and inhibition mechanism. J Agric Food Chem 47: 4121-4125, 1999.
19. Itoh K, Hirata N, Masuda M, Naruto S, Murata K, Wakabayashi K and Matsuda H: Inhibitory effects of *Citrus hassaku* extract and its flavanone glycosides on melanogenesis. Biol Pharm Bull 32: 410-415, 2009.
20. Rodboon T, Okada S and Suwannalert P: Germinated riceberry rice enhanced protocatechuic acid and vanillic acid to suppress melanogenesis through cellular oxidant-related tyrosinase activity in B16 cells. Antioxidants 9: 247, 2020.
21. Kang MS, Lee GH, Choi GE, Yoon HG and Hyun KY: Neuroprotective effect of *Nypa fruticans* wurmb by suppressing TRPV1 following sciatic nerve crush injury in a rat. Nutrients 12: 2618, 2020.
22. Kang MS and Hyun KY: Antinociceptive and anti-inflammatory effects of *Nypa fruticans* wurmb by suppressing TRPV1 in the sciatic neuropathies. Nutrients 12: 135, 2020.
23. Jang TW and Park JH: Anti-inflammatory effects of *Abeliophyllum distichum* nakai (Cultivar Okhwang 1) callus through inhibition of PI3K/Akt, NF-κB and MAPK signaling pathways in lipopolysaccharide-induced macrophages. Processes 9: 1071, 2021.
24. Son KH, Baek JK, Park SB, Kin HN, Park GH, Son HJ, Eo HJ, Song JH, Jeong HJ and Jeong JB: Enhancement of melanin synthesis by the branch extracts of *Vaccinium oldhamii* through activating tyrosinase activity in B16F10 melanoma cells. Korean J Plant Res 31: 547-553, 2018.
25. Jin KS, Oh YN, Hyun SK, Kwon HJ and Kim BW: Betulinic acid isolated from *Vitis amurensis* root inhibits 3-isobutyl-1-methylxanthine induced melanogenesis via the regulation of MEK/ERK and PI3K/Akt pathways in B16F10 cells. Food Chem Toxicol 68: 38-43, 2014.
26. Xie X, White EP and Mehnert JM: Coordinate autophagy and mTOR pathway inhibition enhances cell death in melanoma. PLoS One 8: e55096, 2013.
27. Werzowa J, Koehrer S, Strommer S, Cejka D, Fuereder T, Zebedin E and Wacheck V: Vertical inhibition of the mTORC1/mTORC2/PI3K pathway shows synergistic effects against melanoma in vitro and in vivo. J Invest Dermatol 131: 495-503, 2011.
28. Karbowniczek M, Spittle CS, Morrison T, Wu H and Henske EP: mTOR is activated in the majority of malignant melanomas. J Invest Dermatol 128: 980-987, 2008.
29. Meier F, Schittek B, Busch S, Garbe C, Smalley K, Stayamoorthy K, Li G and Herdyn M: The RAS/RAF/MEK/ERK and PI3K/AKT signaling pathways present molecular targets for the effective treatment of advanced melanoma. Front Biosci 10: 2986-3001, 2005.
30. Costin GE and Hearing VJ: Human skin pigmentation: Melanocytes modulate skin color in response to stress. FASEB J 21: 976-994, 2007.
31. D'Mello SA, Finlay GJ, Baguley BC and Askarian-Amiri ME: Signaling pathways in melanogenesis. Int J Mol Sci 17: 1144, 2016.
32. Boissy RE, Visscher M and DeLong MA: DeoxyArbutin: A novel reversible tyrosinase inhibitor with effective in vivo skin lightening potency. Exp Dermatol 14: 601-608, 2005.
33. Bloom van Staden A, Oosthuizen CB and Lall N: The effect of *Aspalathus linearis* (Burm. f.) R. Dahlgren and its compounds on tyrosinase and melanogenesis. Sci Rep 11: 7020, 2021.
34. Zhang X, Li J, Li Y, Liu Z, Lin Y and Huang JA: Anti-melanogenic effects of epigallocatechin-3-gallate (EGCG), epicatechin-3-gallate (ECG) and gallocatechin-3-gallate (GCG) via down-regulation of cAMP/CREB/MITF signaling pathway in B16F10 melanoma cells. Fitoterapia 145: 104634, 2020.
35. Ramli S and Ruangrungsi N: Tyrosinase inhibition, antioxidant activity and total phenolic content of selected mimosaceae pericarps ethanolic extracts. Int J Pharm 4: 47-57, 2021.
36. Sato K and Toriyama M: Depigmenting effect of catechins. Molecules 14: 4425-4432, 2009.
37. Chen Z, Liang J, Zhang C and Rodrigues CJ Jr: Epicatechin and catechin may prevent coffee berry disease by inhibition of appressorial melanization of *Colletotrichum kahawae*. Biotechnol Lett 28: 1637-1640, 2006.
38. Ohguchi K, Nakajima C, Oyama M, Iinuma M, Itoh T, Akao Y, Nozawa Y and Ito M: Inhibitory effects of flavonoid glycosides isolated from the peel of Japanese persimmon (*Diospyros kaki* 'Fuyu') on melanin biosynthesis. Biol Pharm Bull 33: 122-124, 2010.
39. Balogun TA, Ipinloju N, Abdullateef OT, Moses SI, Omoboyowa DA, James AC, Saibu OA, Akinyemi WF and Oni EA: Computational evaluation of bioactive compounds from *Colocasia affinis* schott as a novel EGFR inhibitor for cancer treatment. Cancer Inform 20: 11769351211049244, 2021.
40. Wang W, Mao S, Yu H, Wu H, Shan X, Zhang X, Cui G and Liu X: *Pinellia pedatisecta* lectin exerts a proinflammatory activity correlated with ROS-MAPKs/NF-κB pathways and the NLRP3 inflammasome in RAW264.7 cells accompanied by cell pyroptosis. Int Immunopharmacol 66: 1-12, 2019.

41. An JH, Won HJ, Seo SK, Kim DY, Ku CS, Oh SK and Ryu HW: Utilization of [6]-gingerol as an origin discriminant marker influencing melanin inhibitory activity relative to its content in Pinellia ternata. J Appl Biol Chem 59: 323-330, 2016.
42. Byun EB, Song HY, Mushtaq S, Kim HM, Kang JA, Yang MS, Sung NY, Jang BS and Byung EH: Gamma-irradiated luteolin inhibits 3-isobutyl-1-methylxanthine-induced melanogenesis through the regulation of CREB/MITF, PI3K/Akt and ERK pathways in B16BL6 melanoma cells. J Med Food 20: 812-819, 2017.
43. Hsiao JJ and Fisher DE: The roles of microphthalmia-associated transcription factor and pigmentation in melanoma. Arch Biochem Biophys 563: 28-34, 2014.
44. Du J, Widlund HR, Horstmann MA, Ramaswamy S, Ross K, Huber WE, Nishimura EK, Golub TR and Fisher DE: Critical role of CDK2 for melanoma growth linked to its melanocyte-specific transcriptional regulation by MITF. Cancer Cell Int 6: 565-576, 2004.
45. Buscà R, Berra E, Gaggioli C, Khaled M, Bille K, Marchetti B, Thyss R, Fitsialos G, Larribère L, Bertolotto C, *et al*: Hypoxia-inducible factor 1α is a new target of microphthalmia-associated transcription factor (MITF) in melanoma cells. J Cell Biol 170: 49-59, 2005.
46. McGill GG, Haq R, Nishimura EK and Fisher DE: c-Met expression is regulated by Mitf in the melanocyte lineage. J Biol Chem 281: 10365-10373, 2006.